Chalcogenide Letters Vol. 12, No. 7, July 2015, p. 363 - 373

OPTICAL PROPERTIES OF PbS CRYSTALS OBTAINED ON GLASS SUBSTRATE FROM SOLUTIONS CONTAINING HYDROXYLAMINE HYDROCHLORIDE IN AN ULTRASONIC BATHS

V. POPESCU[a], A. MOLEA[a], A. DINESCU[b], C. RUSU-TRIŞCĂ[b],
M. MOLDOVAN[c], G. L. POPESCU [a,*]
[a] *Technical University of Cluj-Napoca, 103-105 Muncii Avenue, 400641 Cluj-Napoca, Romania*
[b.] *National Institute for Research and Development in Microtechnologies, IMT, 077190 Bucharest, Romania.*
[c] *"Raluca Ripan" Institute of Chemistry, 30 Fântânele street, 400294 Cluj-Napoca, Romania*

Optical properties of PbS crystals obtained by Chemical bath deposition (CBD) and ultrasonic chemical bath deposition (US-CBD) on glass substrates have been studied. Ultrasounds determined an increase of reflectance, refraction index, real and imaginary parts of dielectric constant, a decrease of absorption coefficient and a red shift of the maxims of absorption coefficient, extinction coefficient and imaginary part of dielectric constant. The bad gaps of the obtained crystals are higher than the values corresponding to bulk PbS both for sample obtained in static and ultrasonic bath. Ultrasounds determined the decreasing of direct band gaps and the increasing of Urbach energy. The changes of optical properties of the sample obtained in sonochemical conditions can be correlated with the increase of the crystallite and grain size.

(Received May 19, 2015, Accepted July 10, 2015)

Keywords: lead sulfide, ultrasounds, optical properties.

1. Introduction

Lead sulfide is a semiconductor with very good absorbing properties in visible and infrared range being an interesting material for applications regarding infrared radiation detection, infrared solar cells, solar control coatings an so on.

One of the most versatile and economic solution for obtaining PbS crystals and films is based on Chemical Bath Deposition (CBD) [1-16] because it doesn't imply expensive and complicate installations and the deposition parameters are easy to control. More than that, the introducing of complexing, surface active, oxidants or reducing agents can influence structural, morphological, electrical and photoelectrical properties of obtained materials.

When CBD is use for films obtaining, the deposition takes places from alkaline baths containing Pb (II) salts and a sulfur compound. In alkaline environment the reaction takes places after an initiation period [11-13] because the reaction between Pb (II) and thiourea (TU) is an autocatalytic one [7].

Sonochemical methods can be applied for increasing the reaction rate in order to decrease the reaction time or to control the morphology of the obtained PbS particles [17-29]. For example Wang et al. obtained PbS cubes, spheres, rods and tubes from solution containing lead acetate or lead nitrate and thioacetamide at a molar ratio of Pb^{2+}/S^{2-} (1:3.16), using cetyltrimethyl ammonium bromide (CTAB) as surfactant [17] in an ultrasonic bath depending on the surfactant concentration, sonication time and lead salt. From solutions containing lead acetate, and small quantity of CTAB, applying 2 hour sonication they obtained irregular cubes. Increasing CTAB

---

[*] Corresponding author: georgepopescu60@gmail.com

concentration they obtained spheres of PbS. At higher surfactant concentration cubes of PbS were formed. If the sonication time has been increased to 4 hours, from solutions containing lead acetate they obtained rods and cubes, while if they used lead nitrate they obtained PbS tubes and cubes [17].

The sonication time influence the shape of the formed crystals. For short sonication time spherical or cubical crystals can be obtained, while for long sonication time the particles joined together and form nanorods [18], nano/microtubes [18, 19] or nanobelts [20].

Apart surface active agents, the solvents used for sonochemical synthesis plays an important role influencing the size and the morphology of the obtained particles [21]. While the use of ethanol promotes the formation of spherical particles with diameters of 1-15 nm, polyethylene glycol determine the formation of particles of 20-30 nm. Water used as solvent assures the formation of cubical particles of 80-100 nm and ethylene glycol favored the formation of large (100-150 nm) cubical crystals, starting from lead acetate and thiourea [21]. Zhao et al. [21] conducted sonication process without cooling so that the temperature reached the boiling points at the end of the reaction.

Another important aspect is the differences between the particles of PbS grown in solution and PbS crystals grown on solid surface like glass. When the formation of PbS took places into solution ultrasounds leads to the decreasing of PbS [27-29] crystallites and the increasing of the band gaps [27,28] while in the case of PbS grown on glass surface the ultrasounds determined the increasing of the size of the crystals [30].

As far as we know, there are no other data in literature related to PbS crystals or films obtaining by sonochemical methods on the surface of glass substrates; although, sonochemical methods were studied to obtain lead sulfide nanoparticles [17-29] or microtubes [19].

Optical properties of PbS films or particles obtained by chemical methods vary in a wide range as a function of crystallite's sizes due to quantum confinement and other factors like surface morphology [6].

When particles sizes decreases the band gap of PbS increase shifting optical response from near infrared region to visible or even to ultraviolet region. The band gap of nanostructured PbS deposited on glass substrate with average crystallites of 40 nm, obtained by Kumar et al [14] by CBD from baths containing lead acetate, NaOH, thiourea, was estimated to 2 eV. When lead acetate was used as Pb^{2+} source, in the presence of NH_3, the obtained band gaps ranged between 1.9 to 2.6 eV, depending on lead salt concentration [15]. In the case of polyvinyl alcohol (PVA) capped nanocrystalline PbS, obtained by CBD [16], the values of direct band gap energy were 2.4–2.81 eV, while the values for indirect transitions the values were 1.24–1.61 eV.

The PbS particles obtained by Indranil Chakraborty had diameters in the range of 1.9–4.1 nm with band gaps from 4.24 to 3.88 eV. Also band gap variation of 3.37 to 2.92 eV has been observed for a variation in particle size from 2.7 to 7.0 nm [31].

The response of PbS has been shifted even further, to near-ultraviolet region up to 5.2 eV varying the size and the shape of the particles obtained by Hoffmann and Entel [32], Thielsch et al [33], Wang [34] and Cao et al. [35].

For this study PbS crystals have been deposited on glass substrate in order to study the initiation of the reaction of formation of PbS films by Chemical Bath Deposition.

Our previous studies showed that US determined the increase of crystallites and grain sizes influencing also the shape of the crystals deposited on glass substrate [30]. This paper presents the study related to the influence of ultrasounds on optical properties of PbS crystals deposited on glass substrate from baths containing hydroxylamine hydrochloride, continuing previous studies [30] regarding the obtaining of PbS in sonochemical conditions [10,30]. We kept all the deposition parameters constant except US, assuring a better temperature control with an improved installation provided with a cooling unit.

2. Experimental details

2.1. PbS crystals deposition on glass substrate

PbS crystals were deposited on glass slides with dimensions of 75x25x1 mm, from baths containing lead nitrate, thiourea and NaOH, using reagents of analytical grade without any purification in the presence of hydroxylamine hydrochloride which assures the formation of uniform films [36] due to the acceleration of the chemical deposition reaction conducting to the decrease in the size of the crystallites [9]. According to [11-13] the chemical reactions that took places between precursors are:

$Pb(NO_3)_2 + 2NaOH \rightarrow Pb(OH)_2 + 2NaNO_3$
$Pb(OH)_2 + 4NaOH \rightarrow Na_4Pb(OH)_6$
$Na_4Pb(OH)_6 \rightarrow 4Na^+ + HPbO_2^- + 3OH^- + H_2O$
$SC(NH_2)_2 + OH^- \rightarrow CH_2N_2 + H_2O + SH^-$
$HPbO_2^- + SH^- \rightarrow PbS + 2OH^-$

In a 150 ml beaker, the deposition solution has been prepared adding in 75 ml water the appropriate amount of lead nitrate solution, under vigorous stirring. In the next step a solution containing NaOH was added dropsied. A white precipitate appears and the precipitate was dissolved when the total amount of NaOH solution was added. Then, a solution containing TU was added to the solution containing lead nitrate and NaOH, followed by the addition of a solution containing hydroxylamine hydrochloride. In the final step water was added until a total volume of 100 ml solution was obtained. The final deposition solutions contains 0.014 M/L lead nitrate, 0.029 M/L thiourea, 0.3 M/L sodium hydroxide and 0.002 m/L hydroxylamine hydrochloride [37].

After preparation the solution was homogenized and then was divided in two 50 ml Berzelius beakers. A microscopic glass slide was introduced in each beaker. One of the beakers was placed in a thermostatic bath (Raypa BOE-2), for static deposition and the other one in an ultrasonic bath (Elma Sonic S 30 H) for deposition under sonochemical conditions at the frequency of 37 kHz. Normally, ultrasounds determine the increasing of the temperature in the solution. In order to avoid the increasing of the temperature under ultrasonic conditions, the bath was cooled using a copper spiral in which cold water was circulated using a Low temperature Bath DC 100 G.

The deposition took places at 35^oC for 40 minutes both in the static (sample CBD) and ultrasonic bath (sample US-CBD).

After deposition, the glass slides with PbS crystals were washed and drayed in an oven for 30 minutes at 60 ^oC, in order to avoid any transformation of the PbS.

2.2. Characterization of PbS crystals deposition on glass substrate

X-ray diffraction (XRD) measurements were performed on a 9 kW triple axis rotating anode Rigaku SmartLab thin film diffraction system (Rigaku Corporation, Japan), powered at U = 45 kV, I = 200 mA. We used in all the measurements the standard thin films X-ray measurement technique, the grazing incidence (GIXRD) method, at a fixed incidence angle of omega = 0.5^o. On the incidence we used the parallel beam mode (PB, divergence 0.05 degrees, incident multilayer mirror). The detector axis (2 theta) was scanned from 15 to 80 degrees with the classical NaI X-ray detector (SC 70, Rigaku) with a continuous scan mode speed of 12 degrees per minute, a scan step of 0.01degrees, $CuK\alpha_{1,2}$ radiation, with no monochromators or filters.

The samples were examined using a field emission **scanning electron microscope** (FE-SEM) – **Raith e_Line** with in-lens electron detection capabilities. In order to avoid the electrostatic charging we used low accelerating voltages and a relatively low beam current.

The transmittance measurements were carried out by using the UV-VIS double beam Spectrophotometer Lambda 35, in the wavelength range 300-1000 nm, using a clean substrate for reference. For diffuse reflectance measurements using an integrated sphere, spectralon reference has been used for calibration.

3. Results and discussions

3.1 Structural and morphological properties

Structural and morphological properties of PbS have been largely discussed in our previous paper [30]. X ray diffraction patterns presented in fig. 1 confirming the formation of PbS crystals (JCPDS card No. 5-592, a=5.936 Å). The average values obtained for crystallites size, were 14.7 nm (static deposition) and 23.6 nm (ultrasonic deposition) respectively, indicating an important increase of the sizes due to ultrasounds [30], while the strain increased from 0.01 to 0.12 % due to the influence of ultrasounds [30].

The lattice constant (a) estimated from the Nelson–Riley plots [30, 38] was a = 5.929 Å for samples CBD and 5.930, for sample US-CBD, which is smaller than the value from the standard card JCPDS No. 5-592 (a_o = 5.936 Å) due to some non-uniform strain of the sample [39].

SEM micrographs (fig. 2) revealed that the grain sizes increases from 183 to 257 nm due to ultrasounds and the shape of the crystals suffered also changes from cubooectadron to cubical one [30].

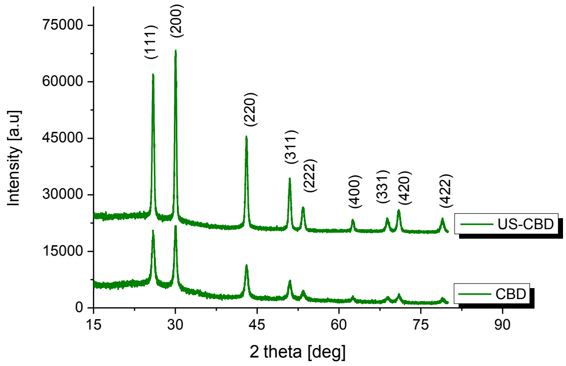

Fig. 1. X-ray diffraction pattern of PbS crystals obtained under static (sample S) and ultrasonic (sample US) conditions on glass substrate [adapted from 30]

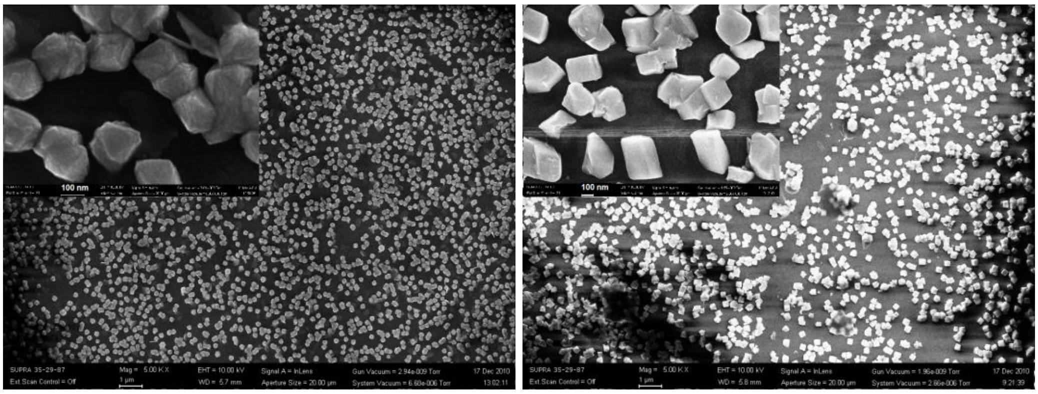

Fig. 2. SEM images of PbS particles deposited on glass substrates by CBD under static (sample CBD column a) and ultrasonic (sample US- CBD column b) conditions [adapted from 30]

3.3. Optical properties

The transmission (T), absorption (A) and reflection (R) spectra of PbS crystals measured after removing the PbS crystals from one side of glass slide are presented in fig. 3.

Since XRD measurements revealed the formation of PbS with no impurities, the difference between the shapes of the transmission spectra were considered to be determined by the difference of crystal sizes and shapes.

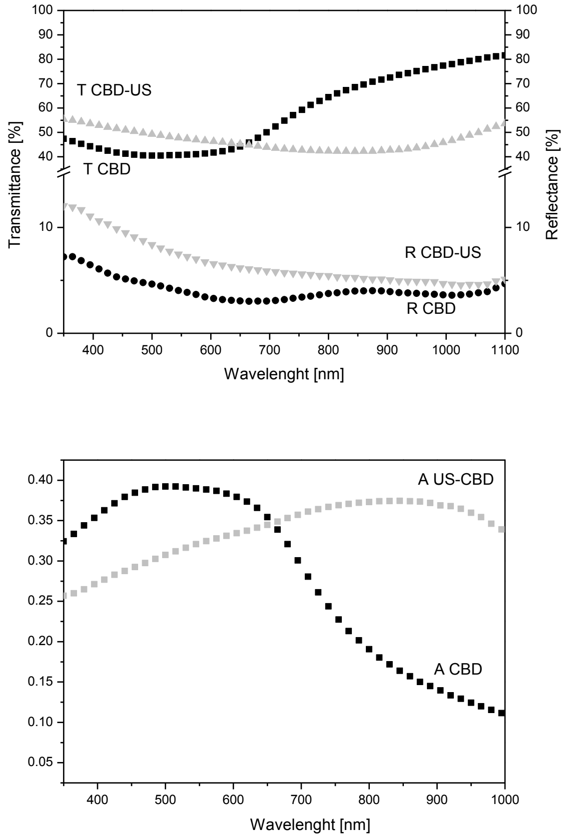

Fig. 3. VIS transmission, reflection (a) and absorption spectra (b) of PbS (samples CBD and US-CBD)

The shape of the transmission spectrum of sample US-CBD is similar with films spectra, while the shape of the spectrum of sample PbS- CBD resemble with PbS nanopowder spectra [14].

As can be observed in figure 3 from absorption spectra, ultrasound resulted in an important red shift of the absorption band from visible (VIS) to Near Infrared (NIR) region. The absorption band position correlated to the size of PbS quantum dots (QDs) was also observed by G. Dong [40] and K.S. Babu [41] et al.-They observed that the absorption band of PbS QDs shifts to the longer wavelength region when the size of the particles increases.

The diffuse reflectance increased for sample CBD-US due to the increase of crystals size and due to plane facets. We can observe in Figure 3 that the reflectance increased up to around 10 % in near ultraviolet region.

Absorption coefficient (α) of the crystals is calculated based on transmittance (T) using the equations:

$$\alpha=(1/h)/\ln(1/T)$$

where h is the light paths (particles sizes).

The plots α=f(nm) are presented in fig. 4 revealing a red shift of α maxims from about 490 nm (sample CBD) to about 850 nm (sample US-CBD). Ultrasound determined a decrease of the values of α for wavelengths smaller than 740 nm followed by an increase toward higher wavelengths.

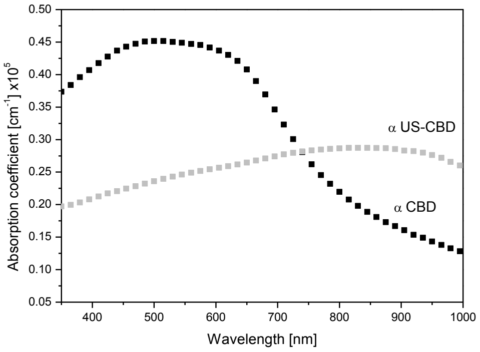

Fig. 4. Absorption coefficient as a function of wavelength for PbS samples (CBD and US-CBD)

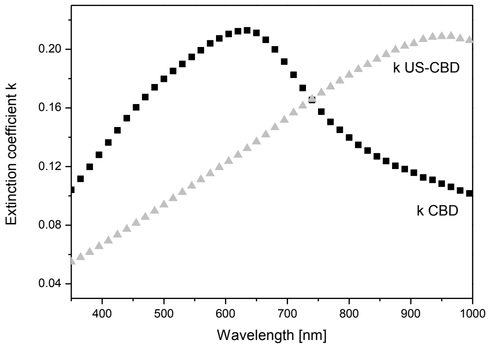

Fig. 5. Extinction coefficient as a function of wavelength for CBD and US-CBD PbS samples

The maximum value of absorption coefficient (0.45×10^5 cm^{-1} for CBD sample and 0.30×10^5 cm^{-1} for US-CBD) is close enough to the values found by other authors who obtained PbS films having a maximum for α of 0.35×10^5 or 0.9×10^4 cm^{-1} [42,43].

Extinction coefficient (k) has been determined based on the relation [44, 45]:

$$k=\alpha\cdot\lambda/4\cdot\pi$$

Fig. 5 presents the dependence of k on wavelength. The maxims of k are around 0.2 for both samples. Ultrasound determined a red shift for extinction coefficient maxims, but the maxims values are almost the same. Our values for k are in the same range with the values obtained by Abbas et al. [42] and Manouchehri [46], but smaller than the one obtained by [47].

The refractive index (n) of PbS was calculated based on the values of the reflectance (R) and k with formula [43,45,48]:

$$n=(1+R/1-R)+((4R/(1-R)^2)-k^2)^{0.5}$$

Bulk PbS and films has high reflective index reaching values up to 5 [42,43,49]. It can be seen in Figure 6 that ultrasounds determined an increase of refractive index for studied wavelengths due to the increasing of the reflectance and particles sizes correlated to the morphology changes. The refractive index values calculated for PbS deposited on glass substrate are smaller than the values corresponding to bulk material. The PbS layer is not continuous and glass substrate has a contribution to the value of the reflectance used for refractive index estimation. When the PbS crystals formed a continuous film on glass substrates the values of refractive index increased up to 3.5 as a function of lead salt concentration [50].

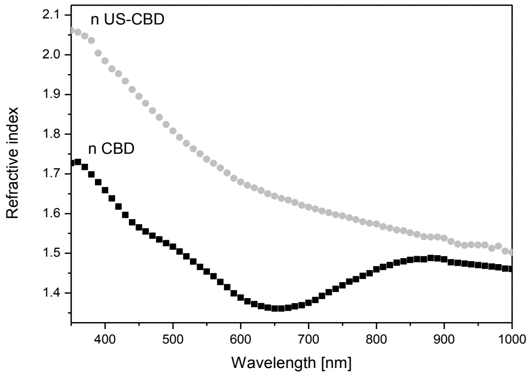

Fig. 6. The dependence of refractive index as a function of wavelength

The real part of dielectric constant $\varepsilon_1 = n^2 - k^2$, the imaginary parts of dielectric constant $\varepsilon_2 = 2n \cdot k$ and the complex dielectric constants $\varepsilon = \varepsilon_{1+}\ \varepsilon_2$ of PbS layers were also estimated [51]. Ultrasound determined a significant increase of ε_1 and ε of PbS crystals (fig. 7) and a red shift of ε_2 maxims (fig. 7 b).

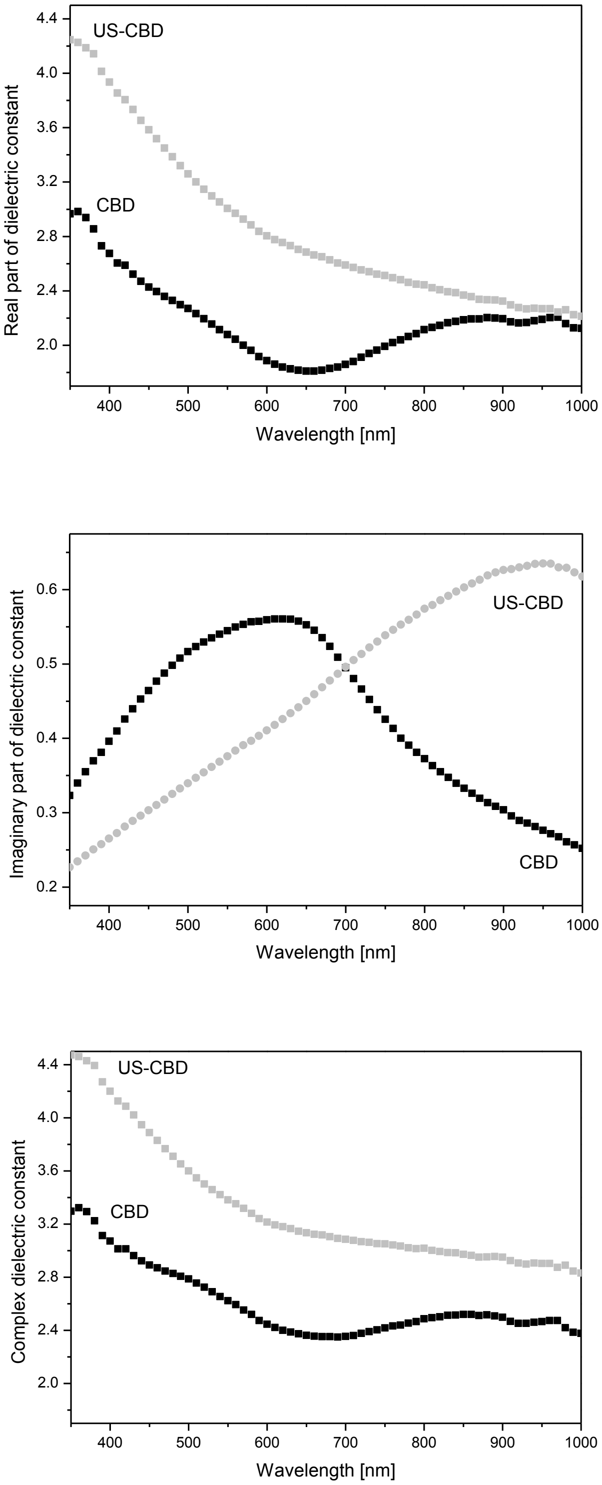

Fig. 7. Real part, imaginary part and complex dielectric constant for PbS crystals as a function of wavelength

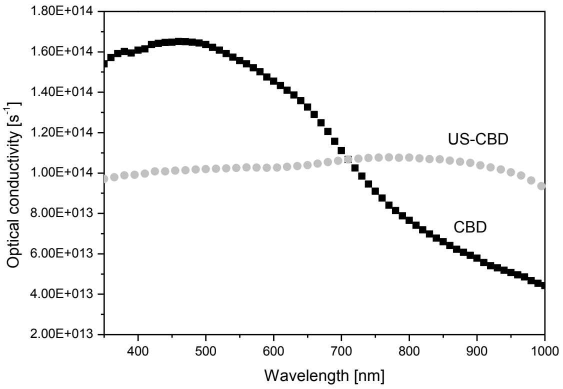

Fig. 8. Optical conductivity of PbS crystals deposited on glass substrate

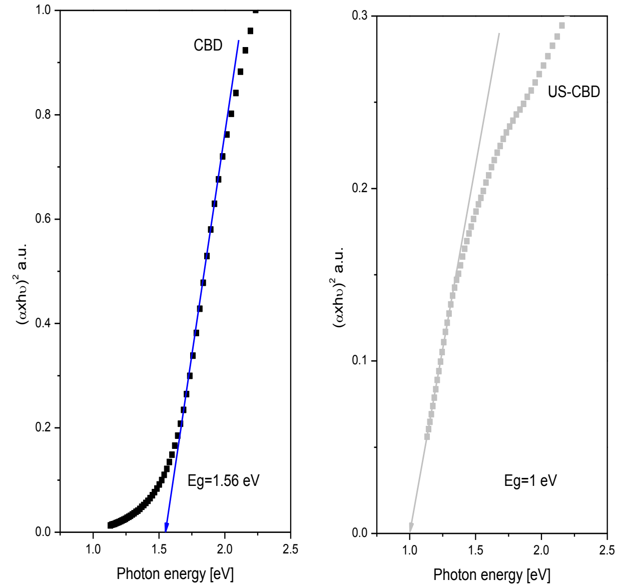

Fig. 9. Tauc plot for the determination of direct band gap of PbS crystals

Optical conductivity was calculated with the relation:

$$\sigma_o = \alpha \cdot n \cdot c/4\pi\ [s^{-1}]$$

where c is the light speed [42,52].

The values of σ_o ranged between 3x10^{13} and 1.6x 10^{14} [s^{-1}] for sample CBD and 7x10^{13} to 1.1x 10^{14} [s^{-1}] for sample US-CBD (Figure 8).

Ultrasound determined the decreasing of optical conductivity for wavelengths smaller than 700 nm and the increasing of optical conductivity for wavelengths higher than 700 nm.

The band gap energy (Eg) was estimated, using Tauc [53] relation:

$$\alpha \cdot h\nu = C(h\nu - E_g)^n$$

where hν is the incident photon energy, C is a constant and n = ½, 2, 3/2 or 3 for allowed direct, allowed indirect, forbidden direct and forbidden indirect electronic transitions.

Optical band gap energy was determined by extrapolating the linear portion of the plot $(\alpha \cdot h\nu)^2 = f(h\nu)$ *[52]* (fig. 9). The direct band gap for sample CBD is around 1.56 eV and the one for US-CBD sample is about 1.02 eV (± 0.02 eV) (table 1) being higher than the bulk band gap value. This increased value of PbS band gap may be explained by surface to volume ratio of the crystals and the less number of atoms in the clusters [14]. The sample obtained under ultrasonic agitation has a smaller band gap due to the increasing of grain size and to decreasing of quantum size effect. Larramendi et al [6] also made an observation related to the influence of surface morphology on the photosensitivity of PbS films and concluded that photoelectric and electric properties of PbS films are mainly determined by the surface and not by the bulk characteristics of the material.

Table 1. Values of optical band gap and Urbach energy for PbS crystals

Sample	Optical Direct $E_{g,d}$ [eV]	Urbach Energy $E_{g,u}$ [eV]
CBD	1.56	0.55
US-CBD	1.02	0.59

Because the absorption coefficients showed an Urbach tail for exponential edge region we calculated Urbach energy (Eu) based on Urbach rule:

$$\alpha = \alpha_o \exp(h\nu/E_U)$$

where α_o is a constant, E_U is the Urbach energy [43]. The equation describes the optical transitions between occupied states in the valence band tail to unoccupied states of the conduction band edge [43].

The value of E_u is obtained from the inverse of the slope of the linear portion of the plot $\ln(\alpha) = f(h\nu)$ of the equation derived from previous relation.

$$\ln\alpha = \alpha_o + h\nu/E_u$$

The Urbach plots and the resulted equations are presented in Figure 10.

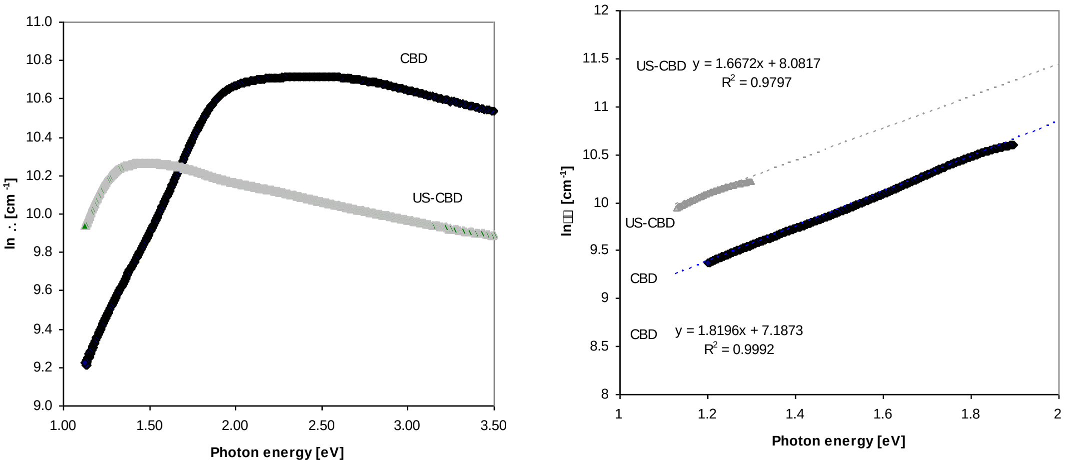

Fig. 10. Urbach plot $\ln\alpha = f(h\nu)$ to determine Urbach energy

The values obtained for E_U are presented in table 1. The increase of crystallites determined by ultrasounds determined the increase of E_U due to crystals defects increasing and to the increased strain of sample US-CBD, comparing to sample CBD. US-CBD contains joined deformed crystals (fig. 2.b).

4. Conclusions

PbS nanostructured depositions on glass substrates have been obtained from static and ultrasonic baths in order to study the influence of ultrasounds on optical properties of the crystals and to correlate optical properties with structural and morphological ones.

Ultrasounds determined an increase of reflectance, refraction index, real and imaginary parts of dielectric constant, a decrease of absorption coefficient and a red shift of the maxims of absorption coefficient, extinction coefficient and imaginary part of dielectric constant.

The bad gaps of the obtained crystals are higher than the values corresponding to bulk PbS both for sample obtained in static and ultrasonic bath. Ultrasounds determined the decreasing of direct band gaps and the increasing of Urbach energy. The changes of optical properties of the sample obtained in sonochemical conditions can be correlated with the increase of the crystallite and grain size.

We demonstrate the possibility of tuning the optical properties of lead sulfide by obtaining the particles in ultrasonic conditions. One can presume that choosing the appropriate exposure to ultrasound radiation one can obtain powders and films of PbS with different optical properties, materials of technological interest for advanced optoelectronic applications, solar control coatings for intelligent windows or infrared solar cells.

References

[1] J.J. Valenzuela-Jáuregui, R. Ramírez-Bon, A. Mendoza-Galván, M. Sotelo-Lerma, Thin Solid Films, **441**(1-2), 104 (2003).
[2] A.A. Rempel, N.S. Kozhevnikova, A.J. G. Leenaers, S. Van Den Berghe, J. Cryst. Growth **280**, 300 (2005).
[3] L. Raniero, C.L. Ferreira, Materials Science Forum **455-456**, 128 (2004).
[4] R.S. Parra, P.J. George, G.G. Sánchez, A.E.J. Gonzalez, L. Baños, P.K. Nair, J. Phys. Chem. Solids, **61**, 659 (2000).
[5] A. Osherov, V. Ezersky, Y. Golan, EPJ Applied Physics, **37**, 39 (2007).
[6] E.M. Larramendi, O. Calzadilla, A. González-Arias, E. Hernández, J. Ruiz-Garcia, Thin Solid, Films, **389**, 301 (2001).
[7] I. Pop, C. Naşcu, V. Ionescu, E. Indrea, I. Bratu, Thin Solid Films, **307**, 240 (1997).
[8] V. Popescu, G. L. Popescu, M. Moldovan, C. Prejmerean, Chalcogenide Lett. **6**, 503 (2009).
[9] E. Pentia, L. Pintilie, I. Matei, T. Botila, E. Ozbaya, J. Optoelectron. Adv. Mater. **3**, 525 (2001).
[10] V. Popescu, N. Jumate, G. L. Popescu, M. Moldovan, C. Prejmerean, Chalcogenide Lett. **7**, 95 (2010).
[11] S. Seghaier, N. Kamoun, R. Brini, A.B. Amara, Mater. Chem. Phys., **97**, 71 (2006).
[12] S.M. Salim, O. Hamid, Renew. Energ., **24**, 575 (2001).
[13] C. Naşcu, I. Pop, V. Ionescu, V. Vomir, Stud. U. Babes-Bol. Che., **37**, 55 (1992).
[14] D. Kumar, G. Agarwal, B. Tripathi, D. Vyas, V. Kulshrestha, J. Alloys Compd., **484**, 463 (2009).
[15] N. Choudhury, B.K. Sarma, Indian J. Pure Ap. Phy., **46**, 261 (2008).
[16] S. Jana, R. Thapa, R. Maity, K.K. Chattopadhyay, Physica E, **40**, 3121 (2008).
[17] S. Fen Wang, F. Gu, M. K. Lu, G. Jun Zhou, A. Yu Zhang, J. Cryst. Growth, **289**, 621 (2006).
[18] Z. Xiu, S. Liu, J. Yu, F. Xu, W. Yu, G. Feng. J. Alloy. Compd., **457**, L9 (2008).
[19] W. Wang, Q. Li, M. Li, H. Lin, L. Hong, J. Cryst. Growth, **299**, 17 (2007).
[20] S. Zhou, X. Zhang, X. Meng, X., Fan, S. Lee, S. Wu, J. Solid State Chem., **178**, 399 (2005).
[21] Y. Zhao, X. Liao, J. Hong, J. & Zhu, Mater. Chem. Phys., **87**, 149 (2004).
[22] R. Xie, D. Li, D. Yang, M. Jiang, M., J. Mater. Sci., **42**, 1376 (2007).
[23] H. Wang, J. Zhang, J. - Zhu, J. Cryst. Growth., **246**, 161 (2002).
[24] J. Zhu, S. Liu, O. Palchik, Y., Koltypin, A. Gedanken, J. Solid State Chem., **153**, 342 (2000).

[25] S. F. Wang, F. Gu, M. K. Lu, Langmuir, **22**, 398 (2006).

[26] S. M., Zhou, Y. S. Feng, L. D. Zhang, J. Mater. Res., **18**, 1188 (2003).

[27] Z. Hosseini, Y. Azizian-Kalandaragh, A. Khodayari, B. Nedaee-Shakarab,

[28] M. Behboudnia, Habibi-Yangjeh, Y. Jafari-Tarzanag, A. Khodayari, Bull. Korean Chem. Soc., **29**, 53, (2008).

[29] A. Phuruangrat, S. Thongtem, T. Thongtem, B. Kuntalue, Dig. J. Nanomater. Bios., **7**, 1413 (2012).

[30] V. Popescu, D. Răducanu, A. Dinescu, M. Dănilă, G. L. Popescu, Chalcogenide Lett., **10**, 5 (2013).

[31] I. P. Chakraborty, S. P. Moulik, J. Nanopart. Res., 7, 237 (2005).

[32] E. Hoffmann, P. Entel, PbS: From Solids to Clusters, http://www.thp.uniduisburg.de/Paper/GK/hoffmann.pdf

[33] R. Thielsch, T. Böhme, R. Reiche, D. Schläfer, H.-D. Bauer, H. Böttcher, Nano Structured Materials, **10**, 131 (1998).

[34] Y. Wang, A. Suna, W. Mahler, R. Kasowski, J. Chem. Phys., **87**, 7315 (1987).

[35] H. Cao, G. Wang, S. Zhang, X. Zhang, Nanotechnology, **17**, 3280 (2006).

[36] E. Pentia, L. Pintilie, C. Tivarus, I. Pintilie, T. Botila, Mat. Sci. Eng. B, **80**, 23 (2001).

[37] C. Naşcu, V. Vomir, V. Ionescu, I. Pop, Rev. Roum. Chim., **40**, 127 (1995).

[38] J.B. Nelson, D.P. Riley, Proc. Phys. Soc., London, **57**, 160 (1945).

[39] N. Choudhury and B. K. Sarma, Thin Solid Films, **31**, 2132 (2011).

[40] G. Dong, B. Wu, F. Zhang, L. Zhang, M. Peng, D. Chen, E. Wu and J. Qiu, J. Alloys Compd., **509**, 9335 (2011).

[41] K.S. Babu, T.R. Kumar, P. Haridoss and C. Vijayan, Talanta, **66**, 160 (2005).

[42] M.M. Abbas, A. Ab-M. Shehab, N-A. Hassan and A-K. Al-Samuraee, Thin Solid Films, **519**, 4917 (2011).

[43] A.A.J. Al-Douri, M.F.A. Alias, M.N. Makadsi, G.H. Mohammed, A.A. Alnajjar, Thin Solid Films, **517**, 881 (2008).

[44] L. Cademartiri, E. Montanari, G. Calestani, A. Migliori, A. Guagliardi, G.A. Ozin, J. Am. Chem. Soc., **128**, 10337 (2006).

[45] J. Solé, L.E. Bausa and D. Jaque, An Introduction to the Optical Spectroscopy of Inorganic Solids, John Wiley & Sons Ltd, England, 2005.

[46] S. Manouchehri et al, The Experiment, **26**, 1816 (2014).

[47] K. C. Preetha, T. L. Remadevi, J. Mater. Sci.: Mater. Electron., **24**, 489 (2013).

[48] A.E. Pop, V. Popescu, A. Dinescu, M. N. Batin, Mater. Sci. Poland, **31**, 318 (2013).

[49] P. Thirumoorthy, P.K. Murali, J. Mater. Sci. Mater. El., **22**, 72 (2011).

[50] Z. Mosiori, Cliff Orori, Njoroge, Walter N., Okumu, John, International Journal of Advanced Research in Physical Science (IJARPS), 1, 25 (2014).

[51] F. Yakuphanoglu, S. Ilican, M. Caglar, Y. Caglar, J. Optoelectron. Adv. Mater. **9**, 2180 (2007).

[52] J.I. Pankove, Optical Processes in semiconductors, Prentice-Hall, New York, 1971.

[53] J. Tauc, Amorphous and Liquid Semiconductors, Plenum Press, London and New York, 1974.

[54] X. Zhao, J. Yu, B. Cheng, Q. Zhang, Colloids Surf. A Physicochem. Eng. Asp., **268**, 78 (2005).